

# Application of scanning tunnelling microscopy to the quality control of tungsten carbide (WC–Co) ball bearings

N. M. D. BROWN, G. M. TAGGART, HONG-XING YOU

*Surface Science Laboratory, Department of Applied Physical Sciences, University of Ulster, Coleraine BT52 1SA, Northern Ireland, UK*

Scanning tunnelling microscopy (STM) has been applied to the topographical study of tungsten carbide (with ~6% Co) ball bearings in air. It is shown that, for this material, scanning tunnelling microscopy can provide not only general topographical information on the surface microtexture with a resolution of nearly 0.1 nm if required, but also quantitative information for the measurement of surface roughness. Thus, scanning tunnelling microscopy has utility as a quality control tool of particular relevance in the submicron range. The STM topographical results from specific tungsten carbide ball bearings are presented, and the limitations and applicability of the STM technique when used as a quality control tool are discussed.

## 1. Introduction

The recent developments in engineering technologies require ever stricter specifications for loaded bearings. It is especially important to ensure the low noise, constant low torque and accuracy qualities of the loaded bearings used in high-precision applications. The measurement and hence control of the surface roughness of load-bearing surfaces is one of the key quality factors needed to meet these requirements. Furthermore, the quality control and process monitoring associated with the need for ever-improved mechanical performance from load-bearing moving surfaces forces the normal optical quality control methods [1] and others, such as stylus profilometry [2] or vibration analysis [3], used for measuring surface roughness to their limits. Indeed, the increasing demand for material processing regimes giving ultra-high standard surface finishes of near-nanometre or better smoothness has generated a world-wide interest in “nanotechnology”. The attendant need for good metrication at this scale of operation is therefore clear.

Scanning tunnelling microscopy (STM) offers uniquely the scale magnification sensitivity required to show surface topographical details down to a resolution of 0.1 nm or better. Such resolution is demonstrably attainable from materials of at least moderate conductivity [4], i.e. metals, alloys, semiconductors, “organic” metals such as charge-transfer complexes and conducting polymers, etc. However, the strength of STM topographical imaging is not restricted to ultra-high resolution at atomic levels. Imaging with a lateral resolution in the submicrometre to nanometre scale is certainly also accessible and of wide potential application. One such branch of STM applications is

the surface roughness measurement of industrially important surfaces [5], where the surface quality, in particular, is a prime requirement. For example, the STM technique has been used for surface roughness measurements of evaporated gold films [6] and gold surfaces [7], sputtered conducting iron oxide films on Si(100) [8], multilayer coated X-ray mirrors [9] and commercial optical recording compact discs [10]. Lateral resolution at ambient pressure in the nanometre range with a vertical stability of about 0.1 nm is now standard with relatively simple STM instrumentation. Moreover, STM imaging is directly applicable, without the need for surface decoration, staining, or replication techniques which, in nanometre-scale scanning or transmission electron microscopy, provide the mass contrast or transparency required.

The work described here is an exploratory application of scanning tunnelling microscopy to the topographical study of the spherical surfaces of tungsten carbide ball bearings and hence, potentially, to their quality control.

## 2. Experimental procedure

The experimental work described here was conducted on tungsten carbide (WC–6% Co) ball bearings of commercial origin (Spheric Engineering, Crawley, West Sussex). These are randomly sampled, 5 mm in diameter with a guaranteed sphericity of  $5 \pm 6.5 \times 10^{-4}$  mm, i.e.  $\langle R \rangle = 2.5 \text{ mm} \pm 325 \text{ nm}$ . The STM system used (W. A. Technology, Cambridge) consists of a conventional X, Y, Z piezo-electric scanning head suitable for use in air or ultra-high vacuum, an electronic control unit, a Tandon 386 microcomputer with VGA colour and monochrome monitors

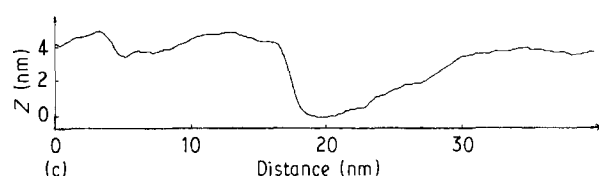
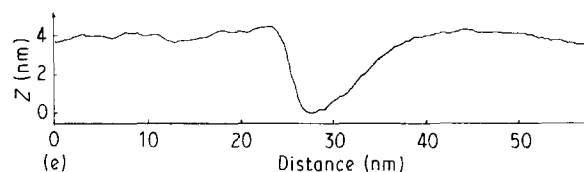
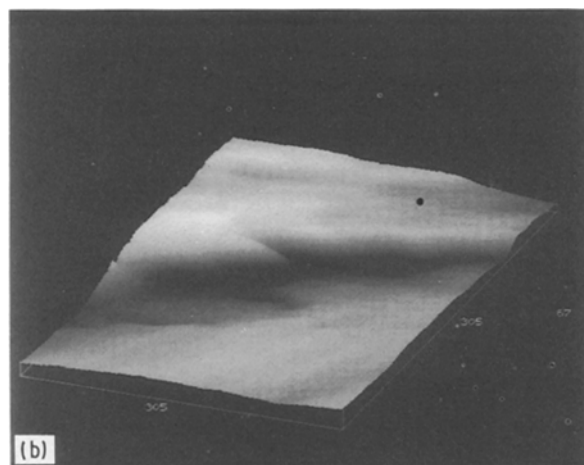
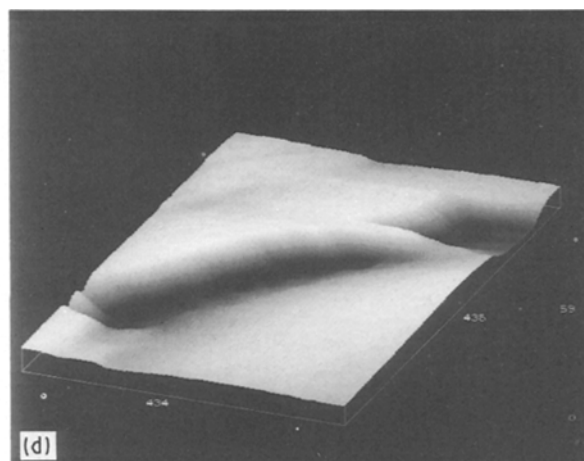
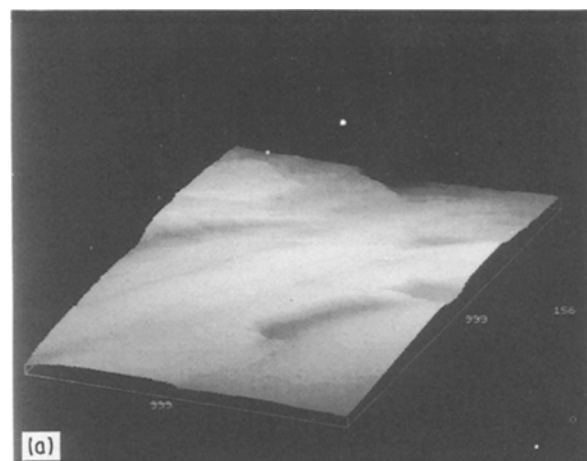


*Figure 1* STM images of a WC-Co carbide ball bearing surface obtained at a bias voltage of 636 mV and a tunnel current of 1.0 nA: (a) three-dimensional topographical image (image size 100 nm  $\times$  100 nm); (b) three-dimensional topographical image of the upper left-hand third of (a) (image size 30.5 nm  $\times$  30.5 nm); (c) line-scan profile from the upper left-hand corner to the lower right-hand corner of the zoomed image (b); (d) three-dimensional topographical image of the lower right half of (a) (image size 43.4 nm  $\times$  43.6 nm); (e) line-scan profile from the upper left-hand corner to the lower right-hand corner of the zoomed image (d).

and a frame store facility. The STM scans in either the  $X$  or  $Y$  direction, as discussed, were recorded in the constant tunnel current mode, i.e. the tunnel current is kept constant via continuous adjustment in the tip height with respect to the sample surface by the electronic feedback loop controlling the  $Z$ -axis piezoelectric actuator as the scan proceeds. The tip thus maps the surface contours of the sample. The typical STM images presented here, in the 80 nm  $\times$  80 nm and 100 nm  $\times$  100 nm ranges, were obtained in air at room temperature from scans of the diamond-polished, as-received, WC-Co carbide ball bearing surfaces. Each image (256  $\times$  256 pixels) was generated in approximately 46 s. The tip used was that produced on a 0.5 mm tungsten wire (99.99%) by routine electrochemical etching in an aqueous 1 M KOH solution [11]. Such tips are reproducibly sharp and well formed, with the tip radii typically  $\sim 0.1 \mu\text{m}$ .

Two kinds of direct quantitative measurement of surface roughness can be made by the STM method. One is the "peak-to-peak" roughness [6, 7, 10], which is measured as the peak amplitude departures from a linear trend line in the STM image data; the other is the r.m.s. surface roughness [8, 9], which is estimated

as the standard deviation from the mean surface plane of the image. In this paper, the mean peak-to-peak roughness over the whole scanned area is then calculated by measuring the peak-to-peak roughness of 256 scanned lines in either the  $X$  or the  $Y$  direction. However, it should be noted that the STM images found are independent of the scan direction. Those shown are obtained directly from the original STM data in that no image processing other than background subtraction was used. In addition, similar images were observed following changes of tips.

### 3. Results

#### 3.1. STM topography

The STM topographical images of the WC-Co carbide ball-bearing surfaces obtained at a bias voltage of 636 mV and a tunnel current of 1.0 nA are shown in Fig. 1a and Fig. 2a, respectively, over scanned areas of 100 nm  $\times$  100 nm. The mean peak-to-peak roughness is  $\sim 11.1$  nm for Fig. 1a and  $\sim 9.1$  nm for Fig. 2. In Fig. 1a, two local "scored" areas can be seen clearly in the surface image. Higher-magnification "zoomed" images of both these areas are represented in Fig. 1b

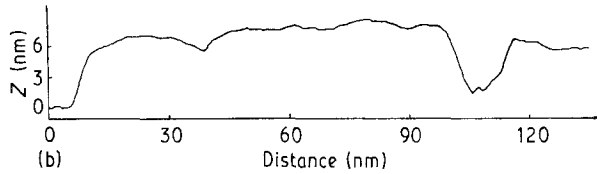
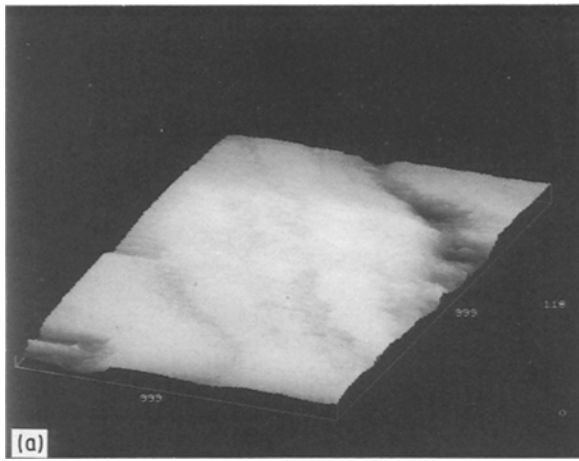


Figure 2 STM image of a WC-Co carbide ball bearing surface obtained at a bias voltage of 636 mV and a tunnel current of 1.0 nA: (a) three-dimensional topographical image (image size 100 nm  $\times$  100 nm); (b) line-scan profile from the upper right-hand corner to the lower left-hand corner of (a).

and d. Also shown in Fig. 1c and e, respectively, are line-scan profiles taken diagonally across the imaged areas from the upper left-hand corner to the lower right-hand corner of these images. These line-scan profiles show that both local faulted areas have a somewhat similar shaped valley, i.e. one steep side and a contrasting gradual slope opposite, with a depth of  $\sim 5.2$  nm. The line-scan profile from the upper right-hand corner to the lower left-hand corner of Fig. 2a is shown in Fig. 2b. From this figure, it is clear that two valleys, one deep ( $\sim 6.0$  nm) and the other shallow ( $\sim 1.5$  nm), are present. A similar shallow valley is also seen in the middle of the image in Fig. 1a. Finally, these various topographical images show that significantly flat surfaces are located between the featured valleys.

Further STM topographical images from the WC-Co carbide ball-bearing sample used, obtained at a bias voltage of 712 mV and a tunnel current of 1.0 nA, are shown in Figs 3a and 4a, respectively, over different scanned areas of 80 nm  $\times$  80 nm. The mean peak-to-peak roughness is found to be  $\sim 14.0$  nm for Fig. 3a and  $\sim 10.3$  nm for Fig. 4a. As shown in Fig. 3a, there is a deep valley passing through the scanned surface in approximately the Y direction, whereas in Fig. 4a a similar surface feature runs diagonally across the scanned surface. By taking line-scan profiles in the X direction at the middle of the front half and the back half of Fig. 3a, the depth and the width of the trough, as plotted in Fig. 3b and c, respectively, are found, i.e. shallower ( $\sim 8.5$  nm) and narrower ( $\sim 28.0$  nm) for Fig. 3b but slightly deeper ( $\sim 10.8$  nm) and wider ( $\sim 36.0$  nm) for Fig. 3c. The line-scan profile across the "scored" area of Fig. 4a in the X direction shows a trench ( $\sim 6.0$  nm deep), as

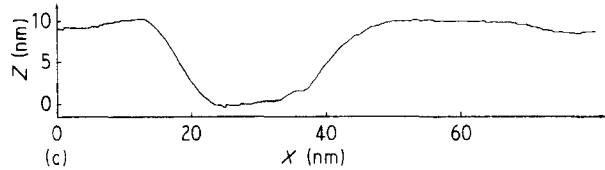
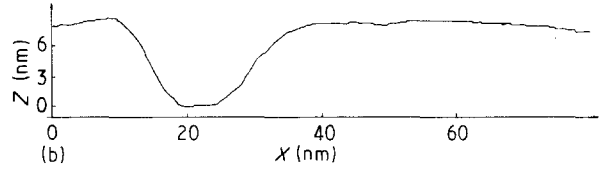
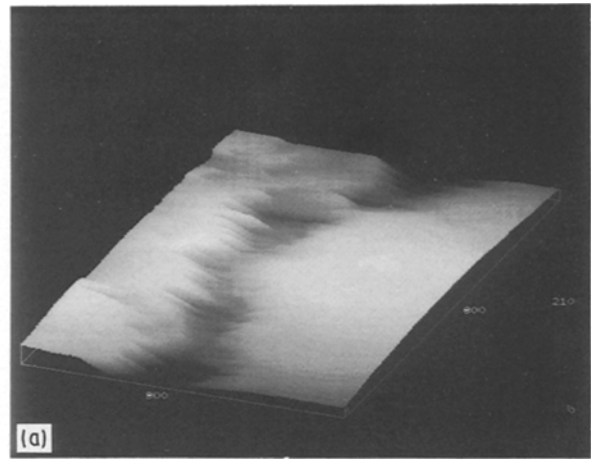


Figure 3 Further STM image of a WC-Co carbide ball bearing obtained at a bias voltage of 712 mV and a tunnel current of 1.0 nA: (a) three-dimensional topographical image (image size 80 nm  $\times$  80 nm); (b) line-scan profile taken at the middle of the front half of (a) in the X direction (from left to right); (c) line-scan profile taken at the middle of the back half of (a) in the X direction.

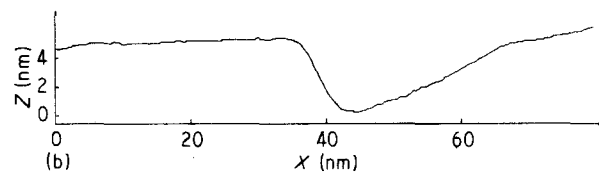
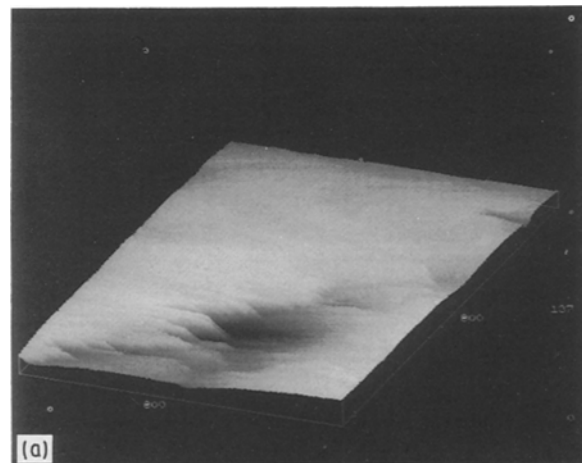


Figure 4 Further STM image of a WC-Co carbide ball bearing obtained at a bias voltage of 712 mV and a tunnel current of 1.0 nA: (a) three-dimensional topographical image (image size 80 nm  $\times$  80 nm); (b) line-scan profile across the scored area in the X direction.

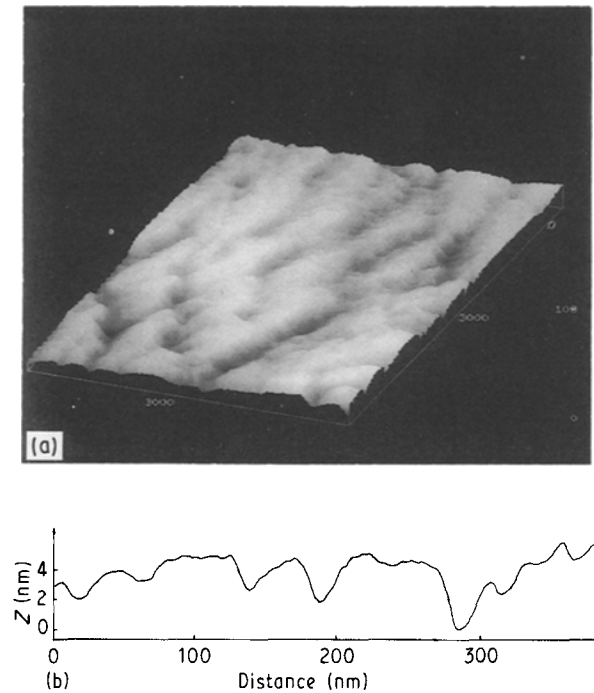


Figure 5 STM image of a WC-Co carbide ball bearing obtained at a bias voltage of 1190 mV and a tunnel current of 1.0 nA over a larger scanned area: (a) three-dimensional topographical image (image size 300 nm  $\times$  300 nm); (b) line-scan profile from the upper left-hand corner to the lower right-hand corner of (a).

indicated in Fig. 4b, similar to that in Fig. 1c and e. In addition, the rest of the surface in Fig. 3a and Fig. 4a, excluding the valley-like regions, is again relatively smooth, with structural features hardly discerned (see also Fig. 3b and c and Fig. 4b), over areas of several square nanometres.

Larger-area STM images have also been scanned on the surfaces of the WC-Co carbide ball bearings. Fig. 5, obtained at a bias voltage of 1190 mV and a tunnel current of 1.0 nA, is typical of those observed over a 300 nm  $\times$  300 nm scan area. The line-scan profile from the upper left-hand corner to the lower right-hand corner of the image is shown in Fig. 5b. The mean peak-to-peak roughness is  $\sim 7.4$  nm. From this image, it can be seen that the broad mounds separated by the troughs identified show relatively flat surfaces. The depth of the troughs, as indicated in Fig. 5b, is changed from  $\sim 1.4$  nm to  $\sim 6.0$  nm. Some of the troughs run in a zig-zag manner across the scanned surface, while some terminate or intersect one with another. These latter surface characteristics, most probably related to the particular sample grinding and polishing procedures used [12], are the most frequently observed topographical features on the larger scanned areas of the WC-Co carbide ball-bearing surfaces studied.

### 3.2. STM roughness measurements

The surface roughness of the WC-Co carbide ball bearing was measured on the different positions by the STM in a series of scanned areas: 20 nm  $\times$  20 nm, 50 nm  $\times$  50 nm, 100 nm  $\times$  100 nm, 150 nm  $\times$  150 nm, 200 nm  $\times$  200 nm, 250 nm  $\times$  250 nm, 300 nm

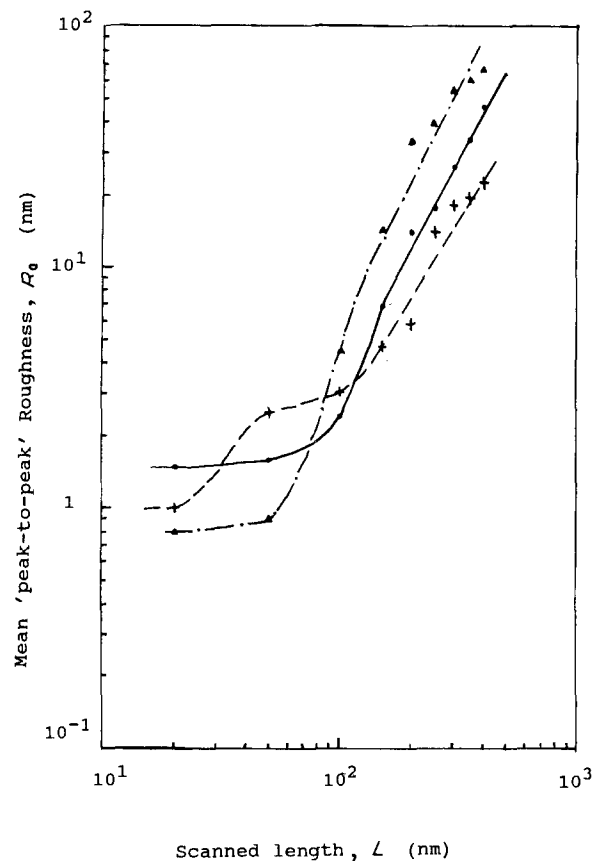


Figure 6 Logarithmic plots of the mean peak-to-peak roughness,  $R_a$ , versus the scanned length,  $L$ , for different positions of the sample: ( $\blacktriangle$ ) position 1, ( $\bullet$ ) position 2, ( $+$ ) position 3.

$\times 300$  nm, 350 nm  $\times$  350 nm and 400 nm  $\times$  400 nm. The mean peak-to-peak roughness was extracted from each STM image. The relationship between the mean peak-to-peak roughness ( $R_a$ ) and the scanned length ( $L$ ) is plotted logarithmically in Fig. 6. As clearly seen in this figure, the plot is almost linear when the scanned area is larger than 100 nm square. According to the standard formula [13], the mean peak-to-peak roughness is given as

$$R_a = A_0 L^D$$

where  $A_0$  is a constant,  $D$  is the topological dimension factor and  $L$  is the length used to determine the scanned area. The values of  $D$  indicate the degree of sample surface finish [9]. For the linear part of Fig. 6, the values of  $D$  are calculated, according to a linear-square regression analysis, to be 2.09, 1.50 and 1.90 for the positions 1, 2 and 3, respectively.

### 4. Discussion

Generally speaking, STM images are a combination of local topographical features and electronic structures. On a scale of tenths of a nanometre, the electronic features of the tip and the sample, in particular, can dominate STM topographical images, but at lower magnifications, i.e. on a nanometre scale, the electronic contributions from the variations, such as in local density of states or local tunnel barrier characteristics, can be neglected [4]. This arises because with average values of the tunnel barrier a change in the

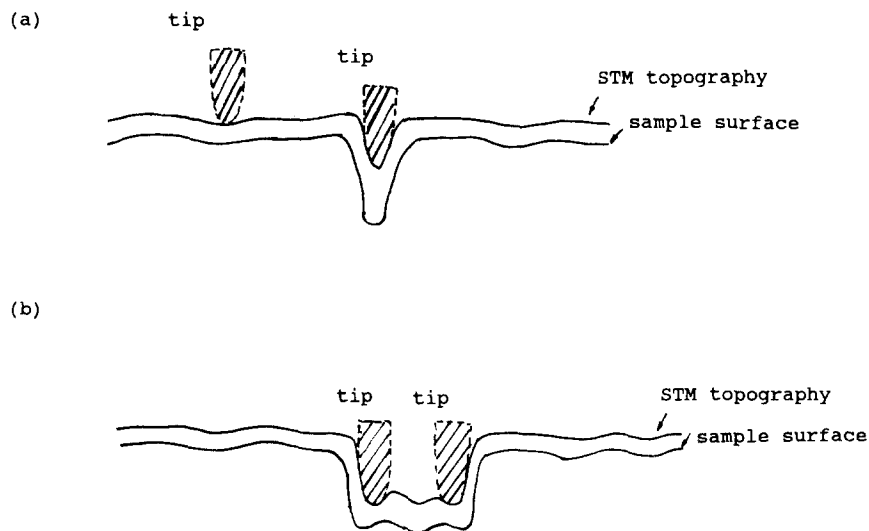


Figure 7 Schematic illustration of the limiting factors in mapping the surface topography of the WC-Co carbide ball bearing: (a) surface with a narrow valley, (b) surface with a wide valley.

effective barrier resistance by a factor of ten corresponds to a displacement of the tip by  $\sim 0.1$  nm [14]. Therefore, the non-linear part of Fig. 6, associated with a dimension below  $\sim 100$  nm, is attributed to the combined effect of the STM topography with the electronic structure, and the STM images presented here are believed to be representative of the topographical structure of the WC-Co carbide ball bearing surfaces.

As far as surface roughness is concerned, one further limitation of the STM technique for making such a measurement should be considered. When scanning on a nanometre scale, STM topographical images are usually a convolution of the local specimen topography and the geometry of the tip [4, 15]. For example, a blunt tip will artificially broaden imaged topographical features and reduce corrugation amplitudes, or the mean peak-to-peak roughness; moreover, the "multiple tip" effects can create "shadows" by fortuitously generating repeated topographical features in the STM image, and the images observed thus reflect distorted rather than genuine surface topography. These phenomena are particularly obvious and severe when the tip is mapping highly corrugated surfaces. Fig. 7 illustrates how the geometry of the tip generally affects the topographical images of the WC-Co carbide ball bearings. As is shown in Fig. 7, for a surface with a narrow valley the measured STM topographical peak (Fig. 7a) is broadened and washed out, and the surface topography found then mainly reflects the shape of the tip rather than the sample surface. On the other hand, for a surface with a wide valley, the measured STM topography (Fig. 7b) correctly represents the sample surface, and the valley floor can be imaged plainly.

The geometry of the tip can therefore play a crucial role in the measurement of surface roughness, especially in the case of narrow and deep structures. For the conventional electrochemical etching used, tungsten tips of  $\sim 0.1$  to  $\sim 0.2$   $\mu\text{m}$  radius are easily achievable, but the surface topography can only be

resolved properly if the effective tip radius is smaller than or comparable to the mean size of the narrow and deep structure. However, with regard to the tip geometry, both the apex and the entire shape of the tip used should be considered. It has been shown by transmission electron microscopy [16] that a tiny cluster usually exists on the end of a tip which has been electrochemically etched. As a result, even though the valley width is less than the overall radius of the tip, the cluster on the apex of the tip acts as the actual point scanning the sample surface, and thus resolves the topographical features which are by comparison shallow and wide, as indicated in Figs 1 to 4. Here, considering the role of the tip geometry in the surface roughness measurement, it should be emphasized that the surface roughness measured by the STM technique is better referred to as the "STM topographical roughness".

With this word of caution, scanning tunnelling microscopy, operated at the nanometre scale, can provide not only surface topographical images of WC-Co carbide ball bearings but also quantitative information for the estimation of the surface roughness. In consequence, scanning tunnelling microscopy can be used as a quality control tool in the detection of the surface microtexture and in the measurement of the surface roughness. Moreover, it offers some significantly operational advantages:

1. It is simple to use, i.e. there are no special sample requirements except that of reasonable sample conductivity and no special sample preparation requirements apart from presenting the sample to the tip. In addition, a scanning tunnelling microscope can be operated in air at atmospheric pressure.
2. There is no mechanical contact between the tip and the sample surface, in contrast with a standard stylus instrument. Consequently, the STM measurement of surface roughness is non-destructive.
3. Scanning tunnelling microscopy offers the highest vertical resolution ( $\sim 0.1$  nm) and lateral resolu-

tion ( $\sim 1.0$  nm) [4, 5, 15] for surface roughness measurements, which is not accessible by any other kind of surface roughness measurement technique.

## 5. Conclusions

Scanning tunnelling microscopy has been used successfully in a topographical study of the spherical surfaces of WC-Co carbide ball bearings. The preliminary STM topographical results presented here show

(i) that the STM technique is applicable to the spherical surfaces of WC-Co carbide ball bearings and to their quality control;

(ii) that, on the nanometre scale, the surfaces of WC-Co carbide ball bearings are reasonably smooth over areas of several square nanometres; and

(iii) that the observed mound structures, related to the sample grinding and polishing procedures, are found to be representative structures of the WC-Co carbide ball bearing surfaces examined.

## Acknowledgements

One of the authors (H. X. Y.) thanks the University of Ulster for a postgraduate studentship. Thanks are also due to the IRCSS at the University of Liverpool for their support.

## References

1. K. NUNOME, M. TSNKAMOTO, T. YATAGAI and H. SATITO, *Appl. Opt.* **24** (1985) 3791.
2. J. M. BENNETT and J. H. DANY, *ibid.* **20** (1981) 1785.
3. H. KANAI, M. ABE and K. KIDO, *J. Acoust. Soc. Jpn* **17** (1986) 343.
4. G. BINNIG and H. ROHRER, *IBM J. Res. Develop.* **30** (1986) 355.
5. N. GARCIA, A. M. BARO, R. MIRANDA, H. ROHRER, Ch. GERBER, R. GARCIA CANTU and J. L. PENA, *Metrologia* **21** (1985) 135.
6. D. R. DENLEY, *J. Vac. Sci. Technol. A* **8** (1990) 603.
7. T. YOKOHATA, K. KATO and K. OHMURA, *ibid.* **8** (1990) 585.
8. C. SCHONENBERGER, S. F. ALVARADO and C. ORTIZ, *J. Appl. Phys.* **66** (1989) 4258.
9. K. NAKAJIMA, S. AOKI, T. KOYANO, E. KITA, A. TASAKI and S. FUJIWAKA, *Jpn. J. Appl. Phys.* **28** (1989) L854.
10. B. A. SEXTON and G. F. COTTERILL, *J. Vac. Sci. Technol. A* **7** (1989) 273.
11. N. M. D. BROWN and HONG-XING YOU, *Surf. Sci.* **233** (1990) 317; **237** (1990) 273.
12. H. MUELLER, K. WETZIG, B. SCHULTRICH, S. M. PIMENOV, N. I. CHAPLIEV, V. I. KONOV and A. M. PROCHOROV, *J. Mater. Sci.* **24** (1989) 3328.
13. ISO/R 468-1966, "Surface Roughness" (International Organization for Standardization, 1966).
14. E. LOUIS, P. ECHENIQUE and F. FLORES, *Physica Scripta* **37** (1988) 359.
15. P. K. HANSMA and J. TERSOFF, *J. Appl. Phys.* **61** (1987) R1.
16. T. TIEDJE, J. VARON, H. DECKMAN and J. STOKES, *J. Vac. Sci. Technol. A* **6** (1988) 372.

*Received 18 June  
and accepted 30 November 1990*